Review article
Perfusion CT: a worthwhile enhancement?

[1,2,3]K A MILES, MD, MSc, FRCR and [2,3]M R GRIFFITHS, BSc, MAppSc

[1]Southernex Imaging Group, Wesley Hospital, Chasely Street, Auchenflower, Queensland 4066, [2]Wesley Research Institute, Wesley Hospital, Chasely Street, Auchenflower, Queensland 4066 and [3]Centre for Medical, Health and Environmental Physics, Queensland University of Technology, George St Brisbane Queensland 4001, Australia

In 1979, just 8 years after Godfrey Hounsfield's introduction of CT, Leon Axel first proposed a method for determining tissue perfusion from dynamic contrast enhanced CT data [1]. Due to the requirement for rapid image acquisition and processing, CT perfusion measurements through the 1980s were largely confined to research studies of renal or myocardial blood flow using electron beam CT systems [2, 3]. However, the advent of spiral CT systems in the 1990s enabled perfusion CT to be performed with conventional CT systems, thereby broadening the technique's availability [4, 5]. The development of multislice CT systems has stimulated further interest by potentially advancing perfusion CT from a single-slice technique to a volume-based examination. More recently, clinical use of CT perfusion imaging has been facilitated by the release of commercial software packages from a range of CT manufacturers. This article aims to review the clinical applications of perfusion CT, discuss the theoretical basis, validation and operation of available software packages and to highlight likely future developments.

Clinical applications

Currently, the major clinical applications of perfusion CT are in acute stroke and oncology. Interestingly, both of these applications have been stimulated by the development of new therapeutic options: thrombolysis in acute stroke and anti-angiogenesis therapy for tumours. The demands on perfusion CT in these two settings are different. In the context of stroke, perfusion is reduced with the aim of therapy being restoration of normal perfusion. To evaluate ischaemic tissue, perfusion values must be related to known ischaemic thresholds, and hence absolute quantification in terms of volume of blood flowing per unit of tissue is essential. On the other hand, tumour perfusion imaging exploits the increase in perfusion that results from tumour neovascularization. However, perfusion in a tumour vascular bed is also affected by cardiac output and thus perfusion parameters that correct for cardiac output may reflect the density of the vascular bed more directly than absolute perfusion values [6].

The use of perfusion CT in these clinical areas is not confined to the selection or monitoring of drug therapy.

Moreover, additional applications also exist in other areas of radiological practice, including nephrology and hepatology. However, when perfusion CT is used for monitoring the effects of therapy, the reproducibility of the technique must be such that the difference between repeated measurements is small relative to the magnitude of the therapeutic change in perfusion. In the context of stroke, an increase of 30 ml min^{-1} 100 g^{-1} will restore the mildest level of ischaemic perfusion to normal [7] and reductions in perfusion due to anti-angiogenesis drug therapy range between 30% to greater than 90% [8, 9]. These changes in perfusion are typically greater than the reproducibility levels of 15–30% reported for perfusion CT.

Acute stroke

Conventional CT is widely used to assess patients suffering acute stroke, primarily to exclude intracerebral haemorrhage. However, approximately 85% of strokes are ischaemic in origin for which, in the majority of patients imaged in the first 6 h, CT is either normal or demonstrates subtle abnormalities that are easy to misinterpret. Perfusion CT can be readily incorporated into the conventional CT assessment of patients with stroke, adding less than 5 min to the imaging time. Experience has shown that non-ionic contrast media can be used safely in this context and the fact that perfusion CT requires only 50 ml of contrast material means that the perfusion image acquisition can be followed by a CT cerebral angiogram to assess patency of the middle cerebral arteries. Thus, a complete imaging evaluation is achievable using widely available equipment whilst avoiding the need to move the patient to another imaging device. The CT perfusion data can positively identify patients with non-haemorrhagic stroke in the presence of a normal conventional CT, provide an indication as to prognosis and potentially select those patients for whom thrombolysis is appropriate. As thrombolysis may only be effective if administered within 3 h to 6 h of ictus [10, 11], the time saved by avoiding additional imaging modalities will be of great value in a situation where rapid treatment decisions are necessary.

Neuronal function is critically dependent upon blood flow and the brain has an intricate system of controls for maintenance of cerebral perfusion. This system of autoregulation is reflected by the perfusion CT findings in patients with cerebral ischaemia (Table 1). Normal cerebral perfusion is approximately 50 ml min^{-1} 100 g^{-1} to 60 ml min^{-1} 100 g^{-1}. A mild reduction in cerebral perfusion pressure is associated with a compensatory dilatation

Table 1. Summary of functional CT findings with worsening ischaemia

	Perfusion	Blood volume	Transit time
Autoregulatory range	N	+	+
Oligaemia (misery perfusion)	−	++	++
Ischaemia (metabolic impairment)	−	+	++
Irreversible damage (necrosis)	− −	−	−/+

N, normal; +, raised; −, decreased.

of cerebral blood vessels. Under these conditions, CT measurements of perfusion remain normal but blood volume and transit time values are increased. As perfusion pressure falls, perfusion can not be maintained at normal levels despite further vasodilatation. When perfusion falls below a threshold of approximately 20 ml min^{-1} 100 g^{-1}, cerebral metabolism is reversibly impaired. However, the development of subsequent irreversible damage, *i.e.* infarction, is also dependent on the time that the tissue has been ischaemic as well as the absolute perfusion value. Irreversible damage is associated with loss of the auto-regulatory vasodilatation and therefore reduced blood volume. Thus, perfusion CT is potentially able to distinguish reversible and irreversible cerebral ischaemia not only by demonstrating more markedly reduced perfusion in areas of infarction but also by exhibiting mismatch between perfusion and blood volume [7, 12]. Reduced perfusion with preserved or increased blood volume implies reversible ischaemia whereas a matched reduction in perfusion and blood volume suggests infarction. Comparison of functional CT images of perfusion and blood volume images may show regions of mismatch implying reversible changes surrounding a region of apparent irreversible infarction (Figure 1). The surrounding reversible region is sometimes referred to as the "penumbra".

Positive identification of non-haemorrhagic stroke with perfusion CT is readily performed using the perfusion or transit time images. It may be clinically useful to distinguish between a completed stroke and transient ischaemic attack (TIA) and occasionally the clinical presentations of stroke and cerebral tumour can be similar. Normal perfusion and mean transit time (MTT) imply a TIA whereas a stroke is seen as a localized area of reduced perfusion and increased MTT (Figure 1). Tumours are typically associated with mildly increased perfusion and normal or reduced MTT, findings that may even occur in low grade tumours that present only subtle signs on conventional CT [7].

The size of the perfusion abnormality in acute stroke can provide an indication of prognosis [13–15]. However, perfusion CT at present is most widely performed using a single or dual slice technique with the chosen slice level passing through the basal ganglia so as to include the vascular territories of the carotid branches that are most frequently affected by thrombosis. Although major ischaemic events will be seen within this slice, it should be remembered that small areas of ischaemia lying outside the slice would not be detected, *e.g.* cerebellar infarcts. Similarly, the extent of infarction may be underestimated.

The ability of perfusion CT to identify areas of salvageable brain tissue indicates a potential role in identifying patients most likely to benefit from thrombolytic therapy aimed at reversing or minimizing ischaemic brain damage. Patients with completed infarction only, as
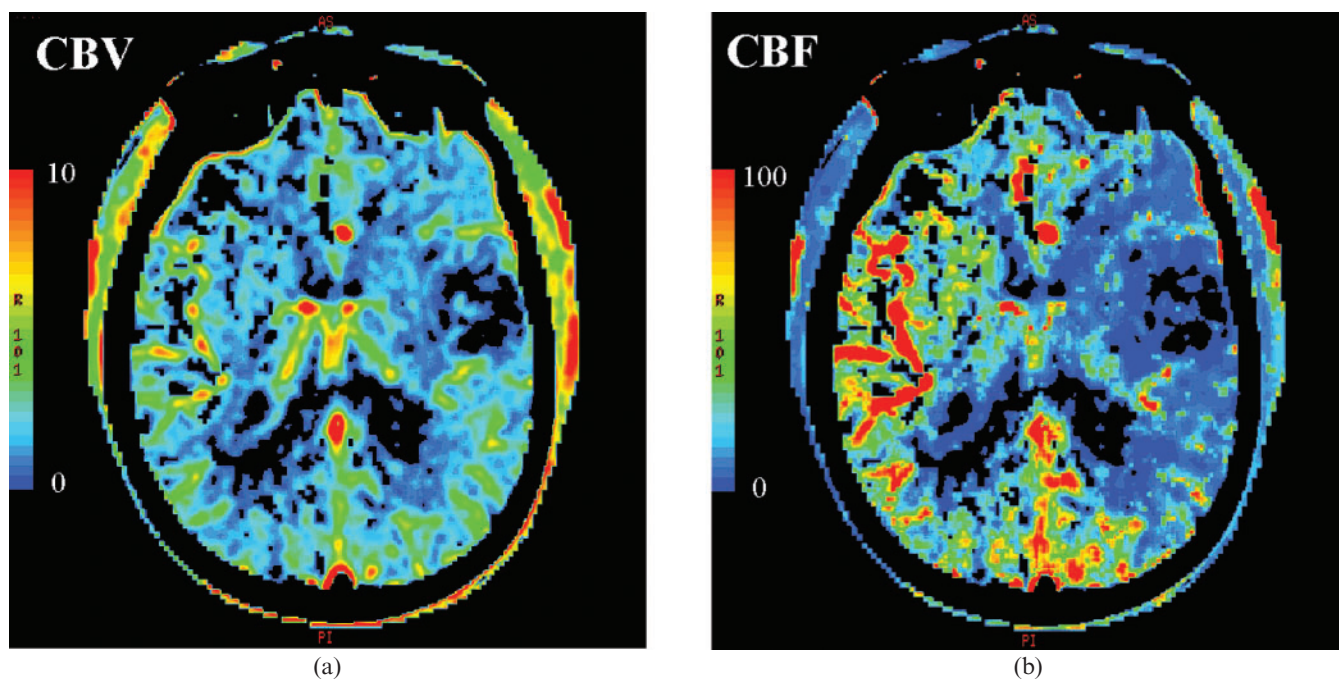

(a)　　　　　　　　　　(b)

Figure 1. Cerebral Perfusion CT. (a) Cerebral blood volume (CBV) and (b) cerebral blood flow (CBF), mismatch post stroke suggestive of extensive penumbra.

indicated by matched reductions of perfusion and blood volume on perfusion CT, could be saved the risks associated with treatment, whereas patients with perfusion/ blood volume mismatch implying reversible damage, would be well suited for therapy. Although the theoretical basis for such an imaging paradigm is attractive, further clinical validation is required.

Oncology

The development of a tumour blood supply through the processes of neovascularization, also known as angiogenesis, is essential for the growth of tumours. Prior to this angiogenesis phase, the size of early tumours is restricted to 2 mm to 3 mm by the lack of access to circulating oxygen, nutrients and growth factors. The development of a blood supply also determines the ability of tumours to metastasize and highly vascularized tumours have been shown to be associated with a poor prognosis for many types of cancer [16, 17]. The basis for the use of perfusion CT in oncology is that the microvascular changes in angiogenesis are reflected by increased tumour perfusion *in vivo* [18]. Indeed, a correlation between contrast enhancement measures and histological assessments of tumour neovascularization such as microvessel density, has been shown for lung and renal cancers with additional tumours currently under investigation [19–21].

CT continues to provide the mainstay for anatomical imaging in oncology. Perfusion CT can be readily incorporated into existing CT protocols, providing information of incremental benefit in diagnosis, staging, assessment of tumour grade and prognosis, and therapy monitoring. Clinical experience to date has largely comprised preliminary series with few large-scale clinical trials, often using semi-quantitative measures of perfusion, such as peak enhancement. However, as it can be shown that enhancement values are indirect measures of perfusion, particularly if the dose of contrast medium is determined from the patient's weight, the results of these studies can be extrapolated to dedicated perfusion CT techniques [6, 22]. The release of commercial software packages can be anticipated to result in wider availability and hence more extensive clinical data, for perfusion CT.

Diagnostic applications of perfusion CT in oncology centre on the distinction of benign from malignant lesions when conventional structural imaging criteria are unreliable. For example, a multicentre trial studying pulmonary nodules that were otherwise indeterminate on conventional CT, demonstrated that peak enhancement of the nodule has a sensitivity of 98% and specificity 58% in the diagnosis of malignancy [23]. Dedicated CT perfusion measurements within lung nodules (Figure 2) have produced similar results [24] and have also been shown to correlate with positron emission tomography (PET) measurements of fluorodeoxyglucose (FDG) uptake, a highly effective but less widely available technique for characterizing pulmonary nodules [6]. By reducing the number of indeterminate CT results, the high negative predictive value of functional CT as an adjunct to a conventional CT examination may lessen the numbers of patients requiring PET, thereby saving on healthcare expenditure.

There is also preliminary evidence that quantification of enhancement within lymph nodes can aid in nodal staging of cancer, where conventional CT, relying on size criteria alone, fails to detect small tumour-bearing nodes and may falsely diagnose enlarged reactive nodes as malignant [25]. Perfusion CT may also improve staging by demonstrating occult hepatic metastases, which remain a significant diagnostic problem despite advances in liver imaging. Perfusion CT can reveal haemodynamic changes in livers bearing experimentally induced metastases with a mean size of only 500 μm [26]. Such flow changes can also be appreciated as increased hepatic parenchymal enhancement during dual-phase spiral CT with increased arterial phase enhancement heralding the subsequent development of overt lesions [27, 28]. Occult hepatic metastases have also been identified as localized areas of high perfusion on CT derived images of hepatic perfusion [29, 30]. However, full analysis of liver perfusion with CT requires separate evaluations of arterial and portal circulations, a functionality that is unavailable with current commercially available software packages.

Although tumour grading is usually undertaken histologically, in heterogeneous tumours biopsies may be subject to sampling error. Imaging techniques, such as perfusion CT that can assess tumour grade *in vivo* can reduce the potential for sampling error by guiding biopsy to the tumour region most likely to be of highest grade. Tumour grading with perfusion CT may also be of value
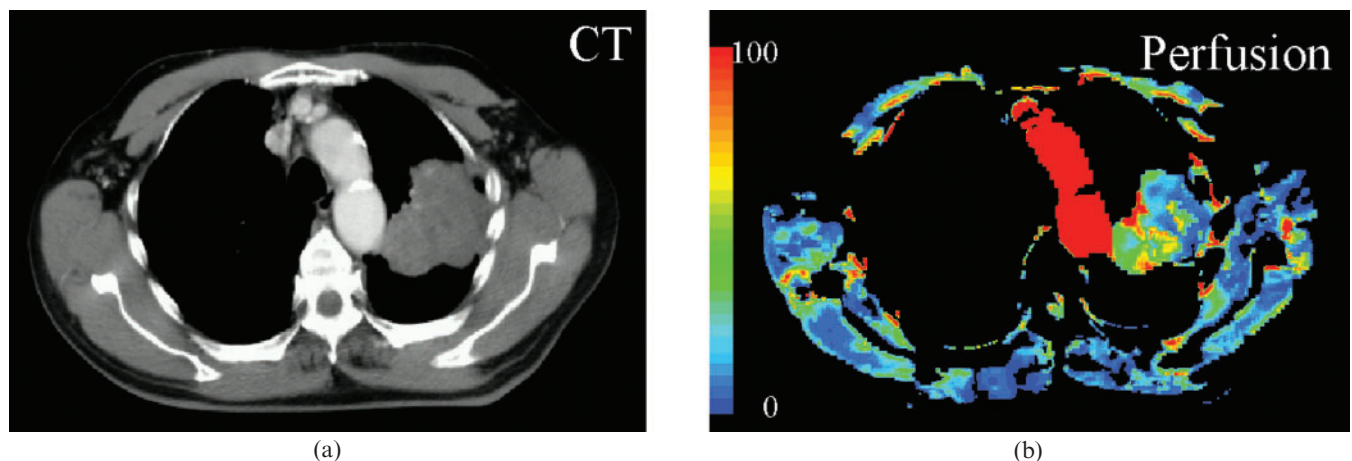

(a) (b)

Figure 2. Perfusion CT of a lung nodule obtained using the deconvolution method. (a) CT image, (b) perfusion image. Note the heterogeneous distribution of perfusion within the nodule.

when biopsy is difficult or when there is a propensity for tumour grade to change with time. In lymphoma, perfusion CT values have been shown to reflect tumour grade with perfusion above 0.5 ml min^{-1} ml^{-1} implying high or intermediate grade tumour [31]. In view of the relatively invasive nature of cerebral biopsy, perfusion CT methods have also been used to assess grade of cerebral glioma. High grade tumours demonstrate increased blood volume values and heterogeneity on blood volume images [32]. There is also potential for CT measurements of blood–brain barrier (BBB) permeability to provide an indication of tumour grade analogous to dynamic contrast enhanced MR techniques [33].

The association between poor prognosis and greater intensity of angiogenesis histologically, is reflected *in vivo* by perfusion CT measurements. CT perfusion values are higher in lung cancers of more advanced stage whilst in head and neck cancer, CT perfusion can identify tumours that are likely to have a favourable outcome following radiotherapy [34]. In patients with hepatic metastases, increased arterial perfusion, particularly in the periphery of the lesion, is associated with longer survival [35]. Preliminary data from patients with metastatic colon cancer suggest that low portal perfusion throughout the liver, *i.e.* below 0.3 ml min^{-1} ml^{-1}, is associated with progressive disease and a poor response to chemotherapy [29, 36]. In the future, such prognostic information could impact upon clinical management, as patients identified to have aggressive tumours may be suitable for additional treatment or invasive local treatments could be withheld when unlikely to be of benefit.

Drug-induced changes in vascular physiology have been measured using functional CT including changes in the permeability of gliomas in response to steroids and the bradykinin analogue RMP-7 [37, 38] and changes in tumour perfusion following BW12C [39] lymphoma chemotherapy [31]. Changes in tumour perfusion and permeability have also been observed following radiotherapy [40, 41]. However, perfusion CT may be of particular value in monitoring the response to emerging "anti-angiogenesis" drugs, which aim to halt cancer progression by suppressing the tumour blood supply. As these agents produce disease stabilization rather than tumour regression, conventional imaging strategies that rely on changes in tumour size are not appropriate [42]. By depicting tumour vascularity in a non-invasive and sensitive manner, perfusion CT offers a novel imaging strategy for monitoring tumour angiogenesis *in vivo*.

Other applications

Perfusion CT has also been applied in a range of additional clinical areas [43]. In hepatology, perfusion CT has been used to evaluate hepatic cirrhosis and liver allografts [4, 44–46]. Cirrhosis is associated with increased arterial perfusion and reduced portal perfusion, with the degree of perfusion change reflecting the severity of liver damage. Portal hypertension is also associated with changes in global and regional splenic perfusion [47]. Within the kidney, not only can CT measure alterations of glomerular filtration [48, 49], it has also been used to demonstrate reduced renal perfusion in hypertension, renal artery stenosis, renal obstruction and cyclosporin toxicity [43, 50–53]. Perfusion CT can also be applied to the pancreas [54]. Although experience in these areas has been limited to date, the increasing availability of commercial perfusion CT software may lead to further development of these applications.

Technical considerations

Effective clinical application of perfusion CT as described above, requires a robust implementation of the technique. The determination of tissue perfusion using CT is based on examining the relationships between the arterial, tissue and potentially the venous enhancement after the introduction of a bolus of contrast material (Figure 3). Repeated rapid CT scans are acquired at the same location to allow determination of time-attenuation curves (TAC). Several methods have been developed for analysing these curves to obtain a perfusion value, some of which have been made commercially available by the major CT vendors. The perfusion methods have been developed from indicator dilution theory (moments method), compartmental analysis (slope method) and a linear systems approach (deconvolution method). The later phases of contrast enhancement can also be analysed to quantify the permeability of capillaries, including the BBB. The theoretical basis for each method is available elsewhere [1, 50, 55–60] and summarized in the appendix.

All the techniques are based on the intravenous administration of iodine based CT contrast material and the fact that the change in attenuation due to this contrast material is directly proportional to the concentration of the contrast material. Thus the enhancement, expressed as a CT number or Hounsfield Unit (HU), can be directly used in tracer based techniques. The series of images obtained as the bolus of contrast material washes into and out of the tissue must contain at least one
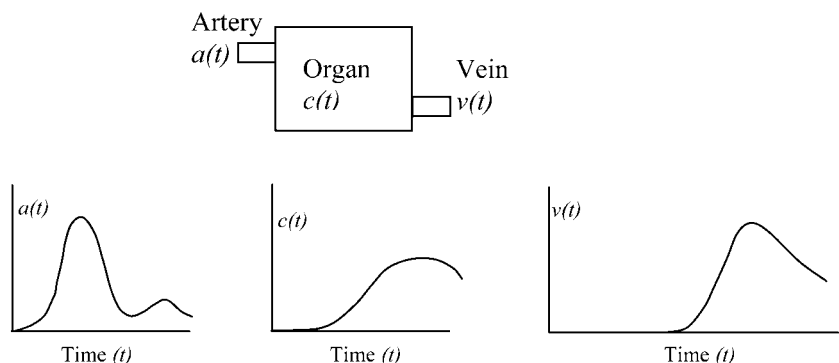

Figure 3. Simple compartment model. Typical arterial, $a(t)$, tissue, $c(t)$, and venous, $v(t)$, time enhancement curves. Note secondary peak in arterial curve due to recirculation.

non contrast-enhanced image to act as a baseline. The baseline image is subtracted either on a pixel by pixel or regional basis, from the remaining image set to obtain time enhancement data. The use of regions of interest allows the generation of organ, regional or pixel time enhancement curves, also termed TACs.

Commercial implementations

Siemens (Erlangen, Germany) have implemented the slope method to calculate perfusion. Blood volume and time to peak enhancement parametric maps are also calculated as well as a temporal maximum intensity projection (tMIP), which provides a maximum enhancement image. The blood volume value is obtained from the ratio of peak tissue enhancement to the peak arterial enhancement. This formulation for blood volume was presented by Koenig [61] and is an approximation of the method of Axel [1], which used the ratio of the areas rather than the maximum enhancements. Time to peak is determined as the time from the arrival of the contrast material in major arterial vessels to the peak tissue enhancement. Partial volume concerns are avoided in cerebral perfusion studies by the suggested use of the superior sagittal sinus as an input. Pixels outside the skull are excluded from analysis. Bone and cerebrospinal fluid pixels are excluded by using threshold HU values. Typical acquisition parameters for cerebral perfusion are a 32 s cine acquisition at 1 image per second with a 10 mm slice thickness at 120 kVp and 210 mA using 50 ml of 370 mg ml^{-1} contrast material injected at 20 ml s^{-1} [61].

The Philips (Best, Netherlands) CT Perfusion package [62] also uses the slope method to calculate perfusion maps, but offers the Mullani–Gould formulation as an option. tMIP image, peak enhancement image, time to peak enhancement and MTT maps can also be calculated. The MTT is calculated as the full width half maximum of the tissue time enhancement curve. Processing requires a region of interest to be placed inside a major artery to generate an arterial time enhancement curve; this curve is smoothed and then used to determine the peak enhancement. Pixel thresholds can be set to exclude air and bone. A major vessel threshold can be set to exclude all pixels above a percentage, *e.g.* 20%, of the peak enhancement. Typical acquisition parameters for cerebral perfusion are a 30 s to 40 s cine with acquisitions every second, (every 2 s as a minimum rate), using 40 ml of contrast material injected at 8 ml s^{-1} with the intention to achieve an enhancement of 6 HU to 8 HU in white matter.

The deconvolution approach has been implemented by G.E. (Milwaukee, USA). This allows calculation of parametric maps for regional blood volume, regional blood flow and MTT. A tumour protocol also allows the calculation of a permeability surface requiring a longer acquisition series to obtain data from the delayed wash out of the interstitial contrast material. Typical acquisition parameters for cerebral perfusion are, a 45 s cine with a 1 s interval, retrospectively reconstructed to a 0.5 s interval, with twin 5 mm slices or a single 10 mm slice acquired at 80 kVp using 190 mAs to 200 mAs. For these acquisition parameters a bolus of 40 ml of 370 mg ml^{-1} strength contrast material injected at 4 ml s^{-1} can be used. The analysis package offers a motion correction for in-plane movement. Cerebral perfusion requires a venous region of interest to scale the arterial time density curve to avoid partial volume problems. Air and bone pixels are excluded from calculations by using HU value thresholds, typically 0 HU to 120 HU.

Validation and reproducibility

The methods for CT perfusion have typically been validated against either microsphere methods in animal studies or stable xenon washout methods in humans. The Moments method has been validated using microsphere measurements of regional cerebral perfusion in dogs [63] and compared with xenon wash out studies in humans [64]. The Mullani–Gould formulation similarly has been validated against microspheres in canine myocardial studies [2, 65, 66]. The slope method has been successfully used and quantitatively validated for abdominal organs and the brain [5, 51, 54, 61, 67–69]. However, the slope method will underestimate the perfusion where the "no venous outflow" assumption is broken, *i.e.* where some contrast material wash out occurs prior to the time of the maximum slope of the tissue TAC. The constrained deconvolution method has been validated against microspheres in studies of rabbit cerebral blood flow [59] and against stable xenon CT in human cerebral studies [70].

Interscan repeatability was assessed by Nabavi et al [71] using the deconvolution method. Repeated cerebral perfusion studies in dogs ($n=4$, two scans each) showed increased variability in white (35%) to grey (31%) matter and from small (34%) to large (26%) regions of interest. Variability of similar magnitude was seen by Cenic et al, also with the deconvolution method, in cerebral perfusion studies in normal rabbits [59] ($n=5$, two or three scans each) and in rabbits (32.5%) with brain tumours ($n=3$, two scans each) (13.2%) [60]. Gillard et al [72], using the slope method, showed little variability in repeated CT perfusion studies in 7 patients 24 h apart ($r=0.88$). This data produced a variability of 13% when re-analysed using the GE deconvolution software (Griffiths MR 2002, personal communication).

Griffiths (preliminary PhD submission, Queensland University of Technology, 1999) showed a good inter-operator reproducibility ($n=43$ patients $r=0.94$) for splenic perfusion calculated using the slope method with an interoperator variability of 8%. Similar interoperator results were reported by Blomley et al [68], using the slope method and electron beam CT, for peak aortic CT number ($r^2=0.99$) and liver slope values ($r^2=0.83$) in 27 and 10 patients, respectively.

Preliminary investigations of the comparability of perfusion values from the slope and GE deconvolution method in lung lesions ($n=16$) and the spleen ($n=20$) showed good correlation ($r=0.86$, $r=0.90$), respectively (Griffiths MR, 2001 personal communication). The slope method showed consistently lower perfusion values than the deconvolution method, however, this may be partially due to the application of a vessel exclusion algorithm in the slope method used. Similar results were observed in a small cerebral perfusion series ($n=6$) where the correlation improved from 0.67 to 0.79 with the vessel exclusion algorithm disabled. Caution is urged in the comparison of results from different methods until there is further standardization or cross calibration of results.

Practical considerations in the application of perfusion CT

Acquisition parameters

CT perfusion studies have been performed at a range of X-ray energies and beam intensities, from 120 kVp at 210 mAs to 80 kVp and 80 mAs. Wintermark et al [73] compared the use of 80 and 120 kVp at 200 mAs on cerebral contrast material enhancement using pre and post enhancement images after a bolus of contrast material. 80 kVp gave increased enhancement, greater contrast between white and grey material and lowered the radiation dose by a factor of 2.8 compared with 120 kVp. The difference in noise between 80 kVp and 120 kVp images was not significant. However, the CT perfusion was not calculated from this data. The radiation dose from a CT perfusion study consisting of a 25 image cine at 2 s intervals using 80 kVp, 200 mAs was 29 mGy absorbed dose to the brain and effective dose of 1.2 mSv [70]. This dose is less than the reference dose for a standard cerebral CT examination (2.5 mSv) but the net dose will vary with acquisition parameters and the number of images.

The slope method requires good contrast material enhancement with minimum noise in those images used to calculate perfusion. However, it generally has a shorter acquisition time and may be able to use acquisition parameters with a greater radiation dose per image. The deconvolution method is not as sensitive to noise in any particular image but in general requires more images. Thus optimum acquisition parameters may have a lower dose per image, but lead to a similar radiation dose due to a greater number of images. There will always be a trade off between radiation dose and increased temporal resolution. The optimal acquisition parameters to provide accurate CT perfusion while minimizing patient radiation dose remain to be determined for each method.

Arterial input

Perfusion CT assumes that the TAC for the vessel in the field of view is the same, with a time shift, as that of the tissue's feeding vessel. This assumption should hold where there is no stenosis between the feeding vessel and the vessel of the imaged tissue and there is no significant circulation from collateral vessels or other circulation abnormalities.

The use of small vessels to obtain the arterial TAC will underestimate enhancement due to partial volume effects. Cenic et al [59] examined the extent of the partial volume effects in a phantom and showed there was negligible effect for arteries with internal diameters greater than 1.73 mm. Many cerebral arteries are smaller than this. CT perfusion applications in the brain generally use enhancement within the sagittal sinus as a measure of the maximum arterial enhancement or to re-scale the arterial time enhancement curve. This approach is reasonable in the brain due to the retention of contrast material within the vascular system by the BBB and the relatively small peak broadening of the bolus during transit through the brain. The use of a venous curve to correct for partial volume effects is not appropriate outside the brain. However, elsewhere in the body an appropriately large artery can often be found on the CT slice.

The slope of the tissue enhancement curve, the time taken to reach the maximum slope and maximum arterial enhancement are dependent on the bolus volume, the rate of injection and the patient's cardiac output. While variations in these parameters have little impact on the deconvolution method, they can affect the slope method. Bell [74] studied the effect of bolus size in radionuclide perfusion studies using the slope method. Significant reduction of perfusion values has been shown with boluses greater than 20 ml when hand injected. This is likely to be due to violation of the no outflow assumption when the bolus is given over too long a period. Perfusion CT uses machine injectors and large cannulae achieving greater injection rates thus minimizing this limitation. Injection rates of up to 20 ml s^{-1} have been previously used in dynamic CT studies [61]. These were well tolerated, although concerns about patient safety have been raised. The optimum bolus size and delivery rate has not been carefully studied in perfusion CT.

Units and corrections

The unit used to express perfusion reflects the area of research in which the application was developed. Traditionally cerebral perfusion has been reported as millilitres of blood per minute per 100 grams of wet tissue, ml min^{-1} 100 g^{-1}, while other applications have used millilitres of blood per minute per millilitre of tissue, ml min^{-1} ml^{-1}. CT perfusion, which is based on the determination of the change of contrast material per voxel or volume element, derives perfusion in ml min^{-1} ml^{-1}. This measurement can be converted to a flow rate per unit mass of tissue by using a value for the physical density of tissue. Typically 1.05 g ml^{-1} is used for brain tissue.

Absolute measurement of perfusion is dependent on the cardiac output at the time of measurement, follow up studies may reflect variations in cardiac output as much as a changed clinical condition. To normalize perfusion values Miles et al [6] has proposed the standardized perfusion value (SPV) as the perfusion scaled by the whole body perfusion, expressed as cardiac output over weight. Cardiac output may be determined from the arterial input TAC provided the dose of contrast material is known.

CT contrast material remains in the extracellular fraction of blood and thus perfusion values may be altered where the haematocrit of the blood in the artery and the tissue differ. A correction for this effect can be applied by scaling the tissue enhancement curve by a factor $\psi = (1-H)/(1-rH)$, where r is the ratio of tissue to artery haematocrit and H the arterial haematocrit [60]. A typical value for r of 0.7 is used in the GE implementation of the deconvolution method. However, this can be adjusted, for example to 0.85 for small infants.

Limitations of perfusion CT

One of the principal limitations of CT perfusion is the limited sample volume. Even with multislice scanners the maximum axial field of view is of the order of 20 mm. This makes the choice of location for the investigation critical as only a limited section of the organ of interest can be studied. Roberts [75] suggested "toggling" the scan table between two locations during the acquisition to allow examination of two separate locations, however the temporal resolution was reduced from 1 s to 5 s. In a study of

9 patients using the deconvolution method they found a single table position would have underestimated or missed blood flow abnormalities in 9 of the 12 patients.

Any movement of the patient during repeated imaging of the same tissue volume over extended periods of time, potentially up to 2 min for permeability studies, will cause errors in the perfusion values. Patient motion entirely within the plane of the image, whether translation or rotation, may be corrected by the use of image registration methods. Patient motion out of the image plane leads to the loss of data, although there may be some limited ability to track moving tissue from slice to slice in multislice studies. Patient motion due to breathing will pose continuing problems for perfusion CT, even with careful instruction of the patient. Miles et al [6] in a study of 16 lung nodules rejected 6 owing to excessive motion or attenuation artefacts. Respiratory gating may ameliorate some of the motion problems, although at the expense of temporal resolution.

Beam hardening artefacts in any of the image set used to determine CT perfusion can have a significant effect on the final perfusion value. The typical tissue enhancement seen in CT perfusion studies is of the order of 10 HU. CT perfusion techniques must be carefully applied where there are attenuation artefacts in the field of view, *e.g.* from prostheses or around anticipated high concentrations of contrast material in the heart.

Future developments

Further development of commercial software can be anticipated with the release of packages for the measurement of liver perfusion and capillary permeability in particular. Packages that calculate the SPV, analogous to the standardized uptake value used in PET [6], would also be advantageous for oncological applications. New image acquisition protocols will enable measurement of multiple physiological parameters in one examination. Development of new contrast agents with longer intravascular residence times may also overcome some of the complexities of physiological modelling required for conventional contrast agents that exhibit two-compartment pharmacokinetics [18].

Application of perfusion CT to multislice systems will enable physiological parameters to be captured over larger tissue volumes, removing the current limitation of a single-slice study generally required for dedicated perfusion and permeability measurements [75]. More sophisticated CT technologies that vary the X-ray exposure during scan rotation may allow reductions in the radiation dose associated with repeated volume acquisitions. Respiratory gating could reduce misregistration artefacts for abdominal functional CT whilst cardiac gating may facilitate measurement of myocardial perfusion.

The advent of integrated PET/CT systems creates opportunities to combine CT perfusion measurements with PET data on glucose metabolism or other physiological processes. One possibility would be to correct PET measurements of FDG uptake for perfusion in order to evaluate FDG tissue extraction more precisely. Combined imaging could also be useful for the *in vivo* investigation of the complex relationship between angiogenesis and glucose metabolism in ischaemic tissue and tumours.

Summary

Perfusion imaging redefines CT as a technique that can now depict vascular physiology in addition to detailed anatomy, a transition that parallels William Harvey's demonstration of the circulatory nature of blood flow at a time when comprehensive knowledge about the structure of the vascular system had existed for centuries. The accumulated data on technical validation and clinical application at this time have reached a critical mass sufficient for equipment manufacturers to offer perfusion CT software packages commercially. Perfusion CT is readily incorporated into the patient's routine CT examination, conferring a worthwhile enhancement to the conventional CT evaluation of acute stroke, cancer and other emerging clinical applications.

References

1. Axel L. Cerebral blood flow determination by rapid-sequence computed tomography: theoretical analysis. Radiology 1980; 137:679–86.
2. Wolfkiel CJ, Ferguson JL, Chomka EV, Law WR, Labin IN, Tenzer ML, et al. Measurement of myocardial blood flow by ultrafast computed tomography. Circulation 1987;76:1262–73.
3. Jaschke W, Sievers RS, Lipton MJ, Cogan MG. Cine-computed tomographic assessment of regional renal blood flow. Acta Radiol 1990;31:77–81.
4. Miles KA, Hayball M, Dixon AK. Colour perfusion imaging: a new application of computed tomography. Lancet 1991; 337:643–5.
5. Miles KA, Hayball MP, Dixon AK. Functional images of hepatic perfusion obtained with dynamic CT. Radiology 1993;188:405–11.
6. Miles KA, Griffiths MR, Fuentes MA. Standardized perfusion value: universal CT contrast enhancement scale that correlates with FDG PET in lung nodules. Radiology 2001;220:548–53.
7. Keith C, Griffiths M, Petersen B, Anderson R, Miles K. Computed tomography perfusion imaging in acute stroke. Australas Radiol 2002;46:221–30.
8. Mullani N, Herbst R, Abbruzzese J, Charnsangavej C, Kim E, Tran H, et al. Antiangiogenic Treatment with Endostatin Results in Uncoupling of Blood Flow and Glucose Metabolism in Human Tumors. Clin Positron Imaging 2000;3:151.
9. Maxwell RJ, Wilson J, Prise VE, Vojnovic B, Rustin GJ, Lodge MA, et al. Evaluation of the anti-vascular effects of combretastatin in rodent tumours by dynamic contrast enhanced MRI. NMR Biomed 2002;15:89–98.
10. Tissue plasminogen activator for acute ischemic stroke. The National Institute of Neurological Disorders and Stroke rt-PA Stroke Study Group. N Engl J Med 1995;333:1581–7.
11. Hacke W, Kaste M, Fieschi C, von Kummer R, Davalos A, Meier D, et al. Randomised double-blind placebo-controlled trial of thrombolytic therapy with intravenous alteplase in acute ischaemic stroke (ECASS II). Second European-Australasian Acute Stroke Study Investigators. Lancet 1998; 352:1245–51.
12. Koenig M, Kraus M, Theek C, Klotz E, Gehlen W, Heuser L. Quantitative assessment of the ischemic brain by means of perfusion-related parameters derived from perfusion CT. Stroke 2001;32:431–7.
13. Mayer TE, Hamann GF, Baranczyk J, Rosengarten B, Klotz E, Wiesmann M, et al. Dynamic CT perfusion imaging of acute stroke. Am J Neuroradiol 2000;21:1441–9.

14. Klotz E, König M. Perfusion measurements of the brain: using dynamic CT for the quantitative assessment of cerebral ischemia in acute stroke. Eur J Radiol 1999;30:170–84.

15. Wintermark M, Reichhart M, Thiran JP, Maeder P, Chalaron M, Schnyder P, et al. Prognostic accuracy of cerebral blood flow measurement by perfusion computed tomography, at the time of emergency room admission, in acute stroke patients. Ann Neurol 2002;51:417–32.

16. Brawer MK, Deering RE, Brown M, Preston SD, Bigler SA. Predictors of pathologic stage in prostatic carcinoma. The role of neovascularity. Cancer 1994;73:678–87.

17. Fontanini G, Lucchi M, Vignati S, Mussi A, Ciardiello F, De Laurentiis M, et al. Angiogenesis as a prognostic indicator of survival in non-small-cell lung carcinoma: a prospective study. J Natl Cancer Inst 1997;89:881–6.

18. Miles KA, Charnsangavej C, Lee FT, Fishman EK, Horton K, Lee TY. Application of CT in the investigation of angiogenesis in oncology. Acad Radiol 2000;7:840–50.

19. Swensen SJ, Brown LR, Colby TV, Weaver AL, Midthun DE. Lung nodule enhancement at CT: prospective findings. Radiology 1996;201:447–55.

20. Tateishi U, Nishihara H, Watanabe S, Morikawa T, Abe K, Miyasaka K. Tumor angiogenesis and dynamic CT in lung adenocarcinoma: radiologic-pathologic correlation. J Comput Assist Tomogr 2001;25:23–7.

21. Jinzaki M, Tanimoto A, Mukai M, Ikeda E, Kobayashi S, Yuasa Y, et al. Double-phase helical CT of small renal parenchymal neoplasms: correlation with pathologic findings and tumor angiogenesis. J Comput Assist Tomogr 2000; 24:835–42.

22. Miles KA. Tumour angiogenesis and its relation to contrast enhancement on computed tomography: a review. Eur J Radiol 1999;30:198–205.

23. Swensen SJ, Viggiano RW, Midthun DE, Muller NL, Sherrick A, Yamashita K, et al. Lung nodule enhancement at CT: multicenter study. Radiology 2000;214:73–80.

24. Zhang M, Kono M. Solitary pulmonary nodules: evaluation of blood flow patterns with dynamic CT. Radiology 1997;205:471–8.

25. Fukuya T, Honda H, Hayashi T, Kaneko K, Tateshi Y, Ro T, et al. Lymph-node metastases: efficacy for detection with helical CT in patients with gastric cancer. Radiology 1995; 197:705–11.

26. Cuenod C, Leconte I, Siauve N, Resten A, Dromain C, Poulet B, et al. Early changes in liver perfusion caused by occult metastases in rats: detection with quantitative CT. Radiology 2001;218:556–61.

27. Platt JF, Francis IR, Ellis JH, Reige KA. Liver metastases: early detection based on abnormal contrast material enhancement at dual-phase helical CT. Radiology 1997;205:49–53.

28. Sheafor DH, Killius JS, Paulson EK, DeLong DM, Foti AM, Nelson RC. Hepatic parenchymal enhancement during triple-phase helical CT: can it be used to predict which patients with breast cancer will develop hepatic metastases? Radiology 2000;214:875–80.

29. Leggett DA, Kelley BB, Bunce IH, Miles KA. Colorectal cancer: diagnostic potential of CT measurements of hepatic perfusion and implications for contrast enhancement protocols. Radiology 1997;205:716–20.

30. Dugdale PE, Miles KA. Hepatic metastases: the value of quantitative assessment of contrast enhancement on computed tomography. Eur J Radiol 1999;30:206–13.

31. Dugdale PE, Miles KA, Bunce I, Kelley BB, Leggett DA. CT measurement of perfusion and permeability within lymphoma masses and its ability to assess grade, activity, and chemotherapeutic response. J Comput Assist Tomogr 1999;23:540–7.

32. Leggett DA, Miles KA, Kelley BB. Blood-brain barrier and blood volume imaging of cerebral glioma using functional CT: a pictorial review. Australas Radiol 1998;42:335–40.

33. Roberts HC, Roberts TP, Brasch RC, Dillon WP. Quantitative measurement of microvascular permeability in human brain tumours achieved using dynamic contrast-enhanced MR imaging: correlation with histologic grade. Am J Neuroradiol 2000;21:891–9.

34. Hermans R, Lambin P, Van den Bogaert W, Haustermans K, Van der Goten A, Baert AL. Non-invasive tumour perfusion measurement by dynamic CT: preliminary results. Radiother Oncol 1997;44:159–62.

35. Miles KA, Leggett DA, Kelley BB, Hayball MP, Sinnatamby R, Bunce I. In vivo assessment of neovascularization of liver metastases using perfusion CT. Br J Radiol 1998;71: 276–81.

36. Sommerfeld N, Miles K, Dugdale P, Leggett D, Bunce I. Colorectal cancer: progressive disease is associated with altered liver perfusion on functional CT. In 50th Annual Meeting of the Royal Australia & New Zealand College of Radiologists. 1999.

37. Yeung WT, Lee TY, Del Maestro RF, Kozak R, Bennett J, Brown T. Effect of steroids on iopamidol blood-brain transfer constant and plasma volume in brain tumors measured with X-ray computed tomography. J Neurooncol 1994;18: 53–60.

38. Ford J, Miles K, Hayball M, Bearcroft P, Bleehan N, Osborn C. A simplified method for measurement of blood-brain barrier permeability using CT: Preliminary results and the effect of RMP-7. In: Faulkner K et al, editors. Quantitative imaging in oncology. London: British Institute of Radiology, 1–5.

39. Falk SJ, Ramsay JR, Ward R, Miles K, Dixon AK, Bleehen NM. BW12C perturbs normal and tumour tissue oxygenation and blood flow in man. Radiother Oncol 1994;32:210–7.

40. Harvey C, Dooher A, Morgan J, Blomley M, Dawson P. Imaging of tumour therapy responses by dynamic CT. Eur J Radiol 1999;30:221–6.

41. Harvey CJ, Blomley MJ, Dawson P, Morgan JA, Dooher A, Deponte J, et al. Functional CT imaging of the acute hyperemic response to radiation therapy of the prostate gland: early experience. J Comput Assist Tomogr 2001;25: 43–9.

42. Li WW. Tumor angiogenesis: molecular pathology, therapeutic targeting, and imaging. Acad Radiol 2000;7:800–11.

43. Miles K, Blomley M. Applications of perfusion CT. In Functional Computed Tomography. Miles K, Dawson P, Blomley M, editors. Oxford ISIS Medical Media, 89–116.

44. Van Beers BE, Leconte I, Materne R, Smith AM, Jamart J, Horsmans Y. Hepatic perfusion parameters in chronic liver disease: dynamic CT measurements correlated with disease severity. Am J Roentgenol 2001;176:667–73.

45. Tsushima Y, Blomley JK, Kusano S, Endo K. The portal component of hepatic perfusion measured by dynamic CT: an indicator of hepatic parenchymal damage. Dig Dis Sci 1999;44:1632–8.

46. Bader TR, Herneth AM, Blaicher W, Steininger R, Muhlbacher F, Lechner G, et al. Hepatic perfusion after liver transplantation: noninvasive measurement with dynamic single-section CT. Radiology 1998;209:129–34.

47. Miles KA, McPherson SJ, Hayball MP. Transient splenic inhomogeneity with contrast-enhanced CT: mechanism and effect of liver disease. Radiology 1995;194:91–5.

48. Miles KA, Leggett DA, Bennett GA. CT derived Patlak images of the human kidney. Br J Radiol 1999;72:153–8.

49. Blomley MJ, Dawson P. Review article: the quantification of renal function with enhanced computed tomography. Br J Radiol 1996;69:989–95.

50. Miles KA. Measurement of tissue perfusion by dynamic computed tomography. Br J Radiol 1991;64:409–12.

51. Miles KA, Hayball MP, Dixon AK. Functional imaging of changes in human intrarenal perfusion using quantitative dynamic computed tomography. Invest Radiol 1994;29:911–4.

52. Blomley MJ, McBride A, Mohammedtagi S, Albrecht T, Harvey CJ, Jager R, et al. Functional renal perfusion imaging with colour mapping: is it a useful adjunct to spiral CT in the assessment of abdominal aortic aneurysm (AAA)? Eur J Radiol 1999;30:214–20.

53. Paul JF, Ugolini P, Sapoval M, Mousseaux E, Gaux JC. Unilateral renal artery stenosis: perfusion patterns with electron-beam dynamic CT-preliminary experience. Radiology 2001;221:261–5.

54. Miles KA, Hayball MP, Dixon AK. Measurement of human pancreatic perfusion using dynamic computed tomography with perfusion imaging. Br J Radiol 1995;68:471–5.

55. Axel L. Tissue mean transit time from dynamic computed tomography by a simple deconvolution technique. Invest Radiol 1983;18:94–9.

56. Mullani N, Gould KL. First pass measurements of regional blood flow using external detectors. J Nucl Med 1983;24:577–81.

57. Patlak CS, Blasberg RG, Fenstermacher JD. Graphical evaluation of blood-to-brain transfer constants from multiple-time uptake data. J Cereb Blood Flow Metab 1983;3:1–7.

58. Gobbel GT, Cann CE, Fike JR. Measurement of regional cerebral blood flow using ultrafast computed tomography. Theoretical aspects. Stroke 1991;22:768–71.

59. Cenic A, Nabavi DG, Craen RA, Gelb AW, Lee TY. Dynamic CT measurement of cerebral blood flow: a validation study. Am J Neuroradiol 1999;20:63–73.

60. Cenic A, Nabavi DG, Craen RA, Gelb AW, Lee TY. A CT method to measure hemodynamics in brain tumors: validation and application of cerebral blood flow maps. Am J Neuroradiol 2000;21:462–70.

61. Koenig M, Klotz E, Luka B, Venderink DJ, Spittler JF, Heuser L. Perfusion CT of the brain: diagnostic approach for early detection of ischemic stroke. Radiology 1998;209:85–93.

62. FUNCTIONAL CT, in Mx8000 Operation Manual, Vol. 2. 2000, Philips Medical Systems. p. 11–1, 11–20.

63. Gobbel GT, Cann CE, Iwamoto HS, Fike JR. Measurement of regional cerebral blood flow in the dog using ultrafast computed tomography. Experimental validation. Stroke 1991;22:772–9.

64. Gobbel GT, Cann CE, Fike JR. Comparison of xenon-enhanced CT with ultrafast CT for measurement of regional cerebral blood flow. Am J Neuroradiol 1993;14:543–50.

65. Rumberger JA, Feiring AJ, Lipton MJ, Higgins CB, Ell SR, Marcus ML. Use of ultrafast computed tomography to quantitate regional myocardial perfusion: a preliminary report. J Am Coll Cardiol 1987;9:59–69.

66. Gould RG, Lipon MJ, McNamara MT, Sievers RE, Koshold S, Higgins CB. Measurement of regional myocardial blood flow in dogs by ultrafast CT. Invest Radiol 1988;23:348–53.

67. Blomley MJ, Coulden R, Bufkin C, Lipton MJ, Dawson P. Contrast bolus dynamic computed tomography for the measurement of solid organ perfusion. Invest Radiol 1993;28 Suppl. 5:S72–7; discussion S78.

68. Blomley MJ, Coulden R, Dawson P, Kormano M, Donlan P, Bufkin C, et al. Liver perfusion studied with ultrafast CT. J Comput Assist Tomogr 1995;19:424–33.

69. Gillard JH, Minhas PS, Hayball MP, Bearcroft PW, Antoun NM, Freer CE, et al. Assessment of quantitative computed tomographic cerebral perfusion imaging with $H_2(15)O$ positron emission tomography. Neurol Res 2000;22:457–64.

70. Wintermark M, Thiran JP, Maeder P, Schnyder P, Meuli R. Simultaneous measurement of regional cerebral blood flow by perfusion CT and stable xenon CT: a validation study. Am J Neuroradiol 2001;22:905–14.

71. Nabavi DG, Cenic A, Dool J, Smith RM, Espinosa F, Craen RA, et al. Quantitative assessment of cerebral hemodynamics using CT: stability, accuracy, and precision studies in dogs. J Comput Assist Tomogr 1999;23:506–15.

72. Gillard JH, Antoun NM, Burnet NG, Pickard JD. Reproducibility of quantitative CT perfusion imaging. Br J Radiol 2001;74:552–5.

73. Wintermark M, Maeder P, Verdun FR, Thiran JP, Valley JF, Schnyder P, et al. Using 80 kVp versus 120 kVp in perfusion CT measurement of regional cerebral blood flow. Am J Neuroradiol 2000;21:1881–4.

74. Bell SD, Peters AM. Measurement of blood flow from first-pass radionuclide angiography: influence of bolus volume. Eur J Nucl Med 1991;18:885–8.

75. Roberts HC, Roberts TP, Smith WS, Lee TJ, Fischbein NJ, Dillon WP. Multisection dynamic CT perfusion for acute cerebral ischemia: the "toggling-table" technique. Am J Neuroradiol 2001;22:1077–80.

Appendix

Indicator dilution theory: moments method

Indicator dilution theory was used by Axel [A1], to develop the basis for the Moments method. Axel showed that, for a non-diffusible tracer, the area under the tissue time density curve divided by the area under the arterial time density curve is the relative tissue volume. The moments method was further refined by Gobbel [A2] who showed that the difference in the centre of gravity of the tissue and arterial time density curves is related to the mean transit time. This allows the calculation of the blood flow as the ratio of the blood volume to mean transit time, Equation (1).

This approach assumes a single pass of contrast material, thus the tissue and artery time attenuation curves (TACs) need to be modelled to remove recirculation effects, typically by using a gamma variate fit [A3]. The moments method does not require any information from a venous TAC.

$$\text{Blood flow} = \frac{\text{blood volume}}{\text{mean transit time}} = n \frac{\dfrac{\text{AUC tissue}}{\text{AUC artery}}}{\langle \text{tissue} \rangle - \langle \text{artery} \rangle} \quad (1)$$

$$\text{where } n = \frac{\left(1 - \text{Hct}_{\text{artery}}\right)\left(1 + k^2\right)}{2\left(1 - r\text{Hct}_{\text{artery}}\right)\left(1 - m\right)}$$

AUC is the area under curve, r is the ratio of tissue to artery haematocrit, $\text{Hct}_{\text{tissue}}/\text{Hct}_{\text{artery}}$, m accounts for difference in contrast material arrival time between the measured artery and the true tissue artery. k is the ratio of the standard deviation of tissue transit times to the mean transit time. The method assumes that the value of k is constant across the tissue. This may not be true for an organ with differing circulation paths.

$\langle \text{tissue} \rangle$ and $\langle \text{artery} \rangle$ are the centres of gravity for the tissue and artery time density curves and are calculated as their first moment, (Equation 2)

$$\langle \text{tissue} \rangle = \frac{\int\limits_0^\infty tc(t)\mathrm{d}t}{\int\limits_0^\infty c(t)\mathrm{d}t} \quad \text{and} \quad \langle \text{artery} \rangle = \frac{\int\limits_0^\infty ta(t)\mathrm{d}t}{\int\limits_0^\infty a(t)\mathrm{d}t} \quad (2)$$

Typical artery and tissue curves are shown in Figure 3. The use of the gamma variate to model these curves also allows calculation of the integral to infinity.

Compartmental analysis

Compartmental analysis is often considered a black box type analysis for the study of the flow of a tracer through a system. The tracer, contrast material in the case of CT, is modelled as entering an organ via an artery and rapidly distributing uniformly within the blood vessels and extracellular space, and then after a short interval starting to leave the organ via a vein. The simplest approach to calculate perfusion is based on the conservation of mass within the system, the Fick Principle, which, in strict form, requires arterial, tissue and venous time concentration curves and is often termed the draining vein assumption method. Perfusion (flow/volume: F/V) is calculated as the concentration of contrast material in the tissue divided by the difference between total amount of contrast material that has flowed into the tissue and the amount of contrast material that has flowed out of the tissue, thus at time t'

$$\frac{F}{V} = \frac{c(t')}{\int_0^{t'} a(t)\mathrm{d}t - \int_0^{t'} v(t)\mathrm{d}t} \qquad (3)$$

where $c(t')$ is the concentration of contrast medium in the tissue at time t', the integrals of $a(t)$ and $v(t)$ from 0 to t' can be calculated as the area under the arterial and venous time attenuation curves. Clearly this method is generally impractical due to the requirement to determine time attenuation data for the artery, tissue and vein from a time series of CT images at a single level. Thus, two methods have been developed that avoid the need for venous measurements by determining tissue and arterial concentrations prior to the time the contrast material starts to flow out of the tissue.

Mullani–Gould formulation

This relationship is variously referred to as the "No Venous Out Flow Method", the "Sapirstein Principle" [A4], the "Single Compartment Formulation" or the "Mullani–Gould Formulation" [A5]. By restricting the time of measurement to prior to the time the contrast starts to flow out of the tissue, the venous term in the denominator of Equation (3) becomes zero.

$$\frac{F}{V} = \frac{c(t')|_{\max}}{\int_0^{t'} a^*(t)\mathrm{d}t} \qquad (4)$$

Typically perfusion is calculated at a time, t', such that $c(t)$ is a maximum, *i.e.* peak tissue enhancement, and $a^*(t)$ is the gamma fit to the arterial curve to correct for recirculation. The method is prone to underestimation of higher values of perfusion as the assumption of "no venous washout" is violated at high flow. Failure to correct the arterial time enhancement curve for recirculation can lead to an over estimation of the area under the curve causing a decrease of perfusion values.

Slope method

The slope method allows calculation of perfusion from a shorter time series and is analogous to a differentiation with respect to time of the Mullani–Gould Formulation (Equation 4). Perfusion (F/V) can be calculated as the maximum slope of tissue enhancement curve divided by the maximum arterial enhancement,

$$\frac{F}{V} = \frac{\frac{\mathrm{d}}{\mathrm{d}t}[c(t)]|_{\max}}{a(t)|_{\max}} \qquad (5)$$

The principle advantage of the slope method is that it allows calculation of the perfusion sooner, as the tissue time enhancement curve reaches its peak gradient well before its peak enhancement value. This reduces the chance of the no venous out flow assumption being broken. The peak arterial enhancement and maximum slope in most tissues occur prior to any recirculation thus avoiding the requirement of curve modelling. The earlier time of perfusion assessment also reduces the likelihood of patient movement and may enable perfusion studies in a single breath hold. However, the slope technique is innately sensitive to noise as the data set is differentiated. Perfusion is effectively calculated from only four images, a baseline, the maximal arterial attenuation image and the two consecutive images displaying the greatest difference in tissue enhancement. Noise in any of these images will directly affect perfusion values.

Linear systems, deconvolution method

The time invariant linear systems model takes quite a different theoretical approach to that used in compartmental models. The method is based on modelling the tissue's impulse response function (IRF) which is the time enhancement curve of the tissue due to an idealized instantaneous injection of one unit of tracer. The IRF can be considered to represent the distribution of transit times in the tissue. The IRF is characterized by an almost instantaneous rise to a plateau, as the contrast material enters and remains within the tissue, which then decays as the contrast material flows out of the tissue. The IRF is sometimes referred to as the impulse residue function, as it characterizes the amount of contrast remaining in the system after a unit bolus. The response function could, in theory, be directly measured by giving a small, fast injection of contrast material directly to the feeding artery of the organ, however, this is generally overly invasive.

The response function from an idealized bolus can be used to determine the response to complex inputs if the system has certain basic properties: (a) Time Invariance; the behaviour after a given injection is independent of the time the injection is administered, (b) Superposition; if an input x_1 causes an output of y_1 and similarly for x_2 and y_2 then an input of x_1+x_2 causes and output of y_1+y_2 and (c) Linearity; if an input of x causes an output of y, then ax causes an output of ay.

A complex input can be considered as a series of scaled and time shifted perfect boluses thus similarly the system's response can be represented as the sum of a correspondingly scaled and time shifted series of responses functions, mathematically this is termed a convolution, represented as $\otimes$, *e.g.* for any generalized system

$$\text{output} = \text{input} \otimes R(t) \qquad (6)$$

where $R(t)$ is the IRF. It was shown by Meier [A6] that the tissue time attenuation curve can be represented as

the perfusion multipled by the arterial time attenuation curve convolved with the impulse response function:

$$c(t) = \frac{F}{V} \cdot a(t) \otimes R(t) \qquad (7)$$

Thus the information about the time shifts and the scaling of the impulse response functions to determine the net tissue response is contained in the perfusion value and the form of the arterial enhancement curve. Hence, Equation 7 can be rearranged as:

$$(t) = a(t) \otimes \frac{F}{V} \cdot R(t) \qquad (8)$$

where the tissue perfusion, F/V, can be considered as a scaling factor for the IRF (Figure 4). Dynamic CT measures the tissue, $c(t)$, and arterial, $a(t)$, time attenuation curves and a de-convolution of these allows the calculation of the perfusion scaled response function, F/V $R(t)$. Perfusion, F/V, can be obtained from the plateau height of the F/V $R(t)$ curve since $R(t)$ at $t=0$ has unit height as it is defined as arising from a unit volume bolus.

The mean transit time can be determined from the area under the $R(t)$ curve divided by the height of the $R(t)$ plateau, [A7]. Since the height of $R(t)$ plateau is normalized to 1, the area under $R(t)$ is the mean transit time. The central volume principle allows calculation of blood volume as blood flow times the mean transit time. Thus the area under the perfusion scaled IRF determined from the deconvolution process gives the Blood Volume, (MTT multiplied by perfusion).

The de-convolution of arterial and tissue TAC can be very sensitive to noise, potentially producing multiple, equally likely mathematical solutions for the IRF. However, many of these are physiologically improbable, *e.g.* requiring rapid and large reversals of blood flow. Typically the deconvolution process is constrained such
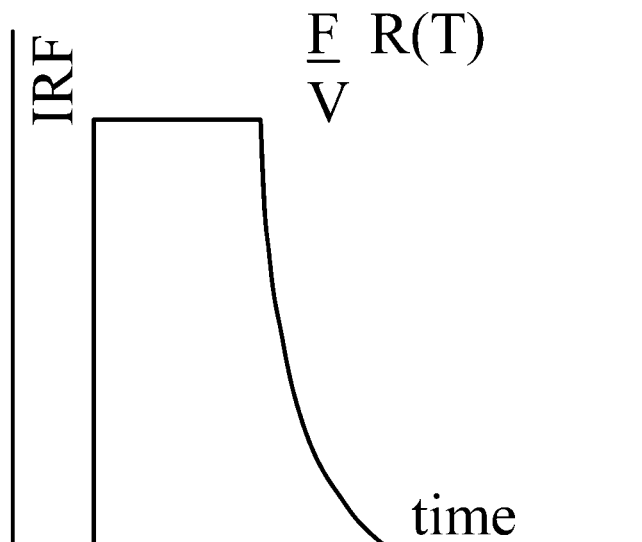

Figure 4. Perfusion scaled impulse response function (IRF). The perfusion (flow over volume) scaled IRF curve initially rises instantaneously to a plateau while all of the contrast material is in the tissue. The length of the plateau is the minimum transit time. The curve will fall to zero as the contrast material is washed out. Perfusion is given by the height of the plateau, the blood volume by the area under the curve. Mean transit time is blood volume divided by the perfusion.

that the derived response function must be positive and smooth with a shape similar to Figure 4 [A8].

The deconvolution method assumes that the contrast material is non-diffusible. While non-diffusibility is a reasonable assumption in the brain, it is not the case for other organs, nor in the case of brain tumour disruption to the blood–brain barrier. Generally, leakage into the interstitial space is slow with respect to the transit time of the contrast material and assuming diffusion is zero only leads to small errors in most organs. Quantitative permeability information can be obtained by the use of Cenic's alteration of the deconvolution method which modelled perfusion in brain tumours as the sum of two IRFs, one owing to intravascular tissue perfusion and the other modelling the flow of contrast material into the extravascular space [A9]. This adaptation allows the deconvolution method to provide permeability values as well as perfusion but requires a longer data acquisition period to determine the outflow characteristics of the extravascular contrast material.

Patlak plot

Quantitative data about the permeability of tissue capillaries, including the blood–brain barrier, can also be obtained using a Patlak plot [A10] in which a two compartment model (blood and tissue extra cellular fluid, ECF) of the dynamic CT data is used.

Consider the oneway transfer of contrast medium from the blood to the ECF with a blood clearance value of contrast, α. The amount of contrast medium that has left the blood will be α times the amount of blood that has flowed through the tissue. The concentration of contrast medium or the enhancement of the ECF will be $\alpha/V \times$ AUC of the blood curve, where V is the volume of the tissue. The enhancement of the tissue due to blood in the tissue is determined by the relative blood volume to tissue volume (rBV) multiplied by the concentration of contrast medium in the blood. Thus the total concentration of contrast medium, *i.e.* enhancement of the tissue at time t' is given by the sum of the concentrations of the contrast medium in the blood and ECF.

$$c(t') = \text{rBV } b(t') + \frac{\alpha}{V} \int_0^{t'} b(t)\mathrm{d}t \qquad (9)$$

Rearranging Equation 9 gives:

$$\frac{c(t')}{b(t')} = \text{rBV} + \frac{\alpha}{V} \frac{\int_0^{t'} b(t)\mathrm{d}t}{b(t')} \qquad (10)$$

which is in the form of $y=mx+c$. Thus, a plot of the ratio of the tissue to blood concentration, $c(t')/b(t')$, against the ratio of the AUC of the blood curve to the blood concentration, $\int_0^{t'} b(t)\mathrm{d}t/b(t')$, for various time values, t', has an intercept of the tissue's relative blood volume and a slope equal to the blood clearance per unit volume or permeability.

Appendix references

A1. Axel L. Cerebral blood flow determination by rapid-sequence computed tomography: theoretical analysis. Radiology 1980;137:679–86.

A2. Gobbel GT, Cann CE, Fike JR. Measurement of regional cerebral blood flow using ultrafast computed tomography. Theoretical aspects. Stroke 1991;22:768–71.

A3. Harpen MD, Lecklitner ML. Derivation of gamma variate indicator dilution function from simple convective dispersion model of blood flow. Med Phys 1984;11:690–2.

A4. Sapirstein LA. Regional blood flow by fractional distribution of indicators. Am J Physiol 1958;193:161–8.

A5. Mullani N, Gould KL. First pass measurements of regional blood flow using external detectors. J Nucl Med 1983; 24:577–81.

A6. Meier P, Zieler K. On the Theory of the Indicator-Dilution Method for the measurement of blood flow and volume. J Appl Physiol 1954;6:731–44.

A7. Axel L. Tissue mean transit time from dynamic computed tomography by a simple deconvolution technique. Invest Radiol 1983;18:94–9.

A8. Yeung WT, Lee TY, Del Maestro RF, Kozak R, Bennett JD, Brown T. An absorptiometry method for the determination of arterial blood concentration of injected iodinated contrast agent. Phys Med Biol 1992;37:1741–58.

A9. Cenic A, Nabavi DG, Craen RA, Gelb AW, Lee TY. A CT method to measure hemodynamics in brain tumors: validation and application of cerebral blood flow maps. Am J Neuroradiol 2000;21:462–70.

A10. Patlak CS, Blasberg RG, Fenstermacher JD. Graphical evaluation of blood-to-brain transfer constants from multiple-time uptake data. J Cereb Blood Flow Metab 1983;3:1–7.